De Novo Discovery of Nonstandard Macrocyclic Peptides as Non-Competitive Inhibitors of the Zika Virus NS2B-NS3 Protease

Christoph Nitsche,[1,#,*] Toby Passioura,[2,#] Paul Varava,[2] Mithun C. Mahawaththa,[1] Mila M. Leuthold,[3] Christian D. Klein,[3] Hiroaki Suga,[2,*] and Gottfried Otting[1]

[1] Research School of Chemistry, Australian National University, Canberra, ACT 2601, Australia

[2] Department of Chemistry, Graduate School of Science, The University of Tokyo, Tokyo 113-0033, Japan

[3] Medicinal Chemistry, Institute of Pharmacy and Molecular Biotechnology IPMB, Heidelberg University, Im Neuenheimer Feld 364, 69120 Heidelberg, Germany

KEYWORDS: *Flavivirus, macrocyclic peptides, protease inhibitors, non-canonical amino acids, display screening.*

ABSTRACT: The Zika virus presents a major public health concern due to severe fetal neurological disorders associated with infections in pregnant women. In addition to vaccine development, the discovery of selective antiviral drugs is essential to combat future epidemic Zika virus outbreaks. The Zika virus NS2B-NS3 protease, which performs replication-critical cleavages of the viral polyprotein, is a promising drug target. We report the first macrocyclic peptide-based inhibitors of the NS2B-NS3 protease, discovered *de novo* through *in vitro* display screening of a genetically reprogrammed library including non-canonical residues. Six compounds were selected, re-synthesized and isolated, all of which displayed affinities in the low nanomolar concentration range. Five compounds showed significant protease inhibition. Two of these were validated as hits with sub-micromolar inhibition constants and selectivity toward Zika over the related proteases from dengue and West Nile viruses. The compounds were characterized as non-competitive inhibitors, suggesting allosteric inhibition.

In recent years, the Zika virus has emerged from a neglected member of the flavivirus genus to a health-threatening pathogen.[1] Although most infections are asymptomatic, neurological complications such as the Guillain-Barré syndrome have been reported in a small proportion of patients. The link between severe disorders in fetuses (microcephaly) and Zika virus infections in pregnant woman prompted the WHO to declare Zika virus a Public Health Emergency of International Concern in 2016.[1, 2] Since then, the virus has circulated in almost all Caribbean and Latin American countries, continental USA (e.g. Florida and Texas), Africa, Southeast Asia, and several Pacific islands with infections reported in 84 countries and territories around the globe. In contrast to other prominent examples of flaviviruses, such as dengue or West Nile, the Zika virus can be transmitted not only by *Aedes aegypti* and *Aedes albopictus* mosquitos, but also through sexual contact.[1, 2] About 30 potential Zika virus vaccines are currently being evaluated, out of which only four have entered phase 1 clinical trials.[2] Particularly concerning for Zika (and dengue) virus vaccination campaigns are potential cross-reactions between Zika and dengue virus antibodies, where the resulting antibody-dependent enhancements can lead to increased viremia and severity of the disease, as observed previously for consecutive infections with different dengue virus serotypes.[2] Therefore, alternative specific antiviral therapeutic options are needed for the treatment of symptomatic patients and infected pregnant women.

Like other flaviviruses, Zika virus comprises a single-stranded positive sense RNA genome that encodes a viral polyprotein, which is post-translationally processed by host-cell proteases and the viral NS2B-NS3 protease into three structural (C, prM/M, E) and seven non-structural proteins (NS1, NS2A, NS2B, NS3, NS4A, NS4B, NS5). The NS2B-NS3 protease of flaviviruses is considered a promising antiviral drug target and several lead compounds have already been discovered for the corresponding dengue virus proteases.[3] NS2B-NS3 is a serine protease, which consists of the N-terminal domain of NS3 and a short cofactor from the hydrophilic core sequence of NS2B. For *in vitro* screening campaigns, three different Zika virus NS2B-NS3 protease (ZIKVpro) constructs have been proposed and crystallized. First, a construct with a covalent linker peptide between NS2B and NS3 (gZiPro) was adopted based on previous successful dengue and West Nile virus protease constructs.[4] Two additional unlinked versions have been described, which are based on either NS2B/NS3 co-expression (bZiPro)[5] or an autocleavage site in the linker peptide between NS2B and NS3 (eZiPro).[6] The C-terminal tetrapeptide of NS2B in eZiPro was shown to interfere with access of substrate to the active site.[6]

Few ZIKVpro inhibitors have been described so far.[7] The most effective ones are substrate-derived peptide analogs that bind covalently to the catalytically active serine residue (e.g. **cn-716**, Figure 2).[4, 8, 9] However, due to conserved features in substrate recognition amongst serine proteases,

these compounds display only poor selectivity between flaviviral and host proteases.[8] Therefore, alternative non-active-site inhibitors that do not mimic the substrate or transition state may exhibit decreased off-target effects. Recently, natural products as well as compounds derived from previous West Nile virus screening campaigns have been reported to act as micromolar allosteric inhibitors of ZIKVpro.[10, 11] In view of the limited coverage of chemical space offered by natural products and compound libraries, as well as common bias for promiscuous binders, we set out to identify completely new structural scaffolds *de novo* by capitalizing on recent advances in mRNA display techniques.

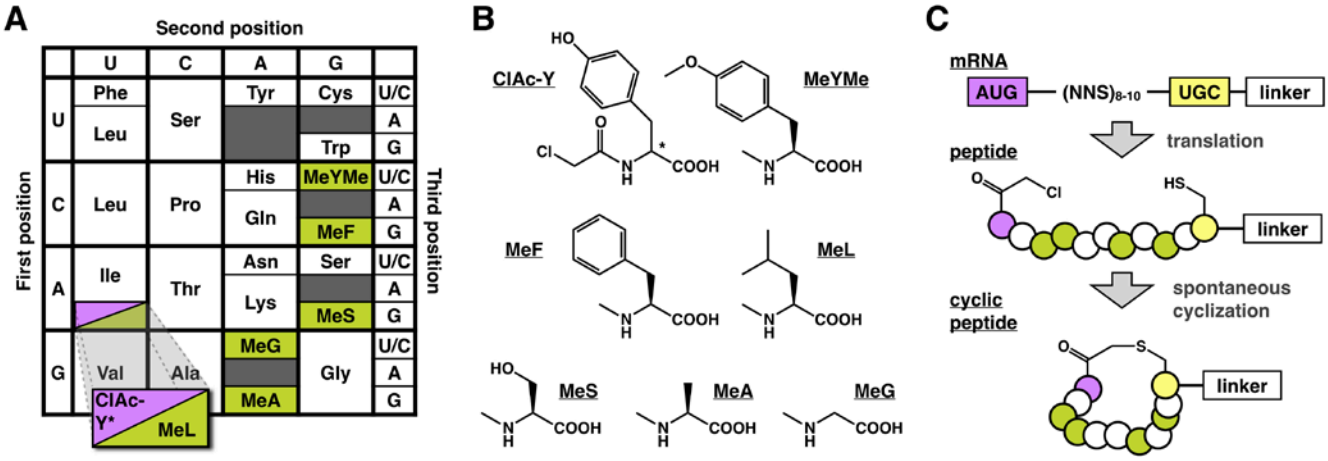

Figure 1. Design of macrocyclic peptide libraries for screening. The peptide libraries for screening were synthesized by genetically reprogrammed translation of a new mRNA library that was more focussed on hydrophobic residues than previous libraries. The codon table for the genetic code used is shown in (**A**) with Met replaced with *N*-chloroacetyl-tyrosine (ClAc-Y) for the initiation AUG codon or *N*-methyl-leucine (^{Me}L) for all downstream AUG codons. **B**: Structures of the non-canonical amino acids used. **C**: The peptide libraries were synthesized by translation of a semi-random mRNA template comprised of an AUG start codon, 8-10 NNS codons (N = A, G, C or U; S = G or C), a UGC (Cys) codon, and a linker sequence for covalent linkage of each peptide and mRNA. Translation of this library under the genetic code shown leads to formation of a semi-randomized peptide library that cyclizes spontaneously to produce a macrocyclic peptide library. * Two libraries were synthesized, one initiated with ClAc-L-Y and one initiated with ClAc-D-Y.

Small (< 2 kDa) macrocyclic peptides are appealing starting points for such drug discovery. A key strength of macrocyclic peptides is that high-affinity ligands can be isolated for nearly any target rapidly using display screening approaches (phage display, mRNA display, etc.).[12] Moreover, display screening can be combined with genetic code reprogramming techniques, allowing the screening of libraries incorporating structural characteristics such as backbone N-methylation and/or D-stereochemistry, which have been shown to improve biostability and membrane permeability, and therefore making the resulting hit compounds better starting points for drug discovery efforts than canonical peptides.[12-14] In the present study, we have used such a screening approach (Random non-standard Peptide Integrated Discovery, RaPID – Figure S1) to identify potent macrocyclic peptide ligands of ZIKVpro. These peptide ligands were specific non-competitive inhibitors for ZIKVpro, and several were found to display sub-micromolar inhibition constants (K_i). This study highlights the ability of such screening approaches to rapidly identify potent inhibitors of newly discovered targets such as those from emerging viral diseases.

In order to identify novel inhibitors of ZIKVpro, we designed two macrocyclic peptide libraries for affinity screening by RaPID display. The libraries were constructed using a genetically reprogrammed *in vitro* translation approach and were designed to include five *N*-methyl residues (^{Me}G, ^{Me}L, ^{Me}A, ^{Me}S, ^{Me}F) and the unnatural amino acid *N*-methyl-4-*O*-methyl-tyrosine ($^{Me}Y_{Me}$) (Figure 1, A and B). Each library was initiated with either L- or D-*N*-chloroacetyl tyrosine, in order to induce spontaneous macrocyclization following translation (Figure 1C).[15] The genetic code was designed such that the non-canonical amino acids replaced Met (allowing for reprogramming of translation initiation) and all of the canonical residues except Lys which have charged side chains at neutral pH (i.e. Asp, Glu, and Arg). Additionally, the random region of the peptide library was limited to a maximum of 10 codons, making the overall library both less charged and smaller than any previously reported comparable cyclic peptide libraries.[12, 13, 16-21] The total theoretical diversity of both libraries combined exceeded $5 \cdot 10^{13}$ macrocyclic peptides, making the total number of compounds screened several orders of magnitude greater than is typical using conventional high-throughput methods.

Iterative affinity screening of these libraries against the linked ZIKVpro construct (gZiPro) immobilized on magnetic beads led to the identification of six families of macrocyclic peptide ligands (alignments of the 100 most frequent sequences from each library are shown in Figure S2). The most abundant member of each of these was synthesized by solid phase methodology omitting the C-terminal linker sequence (i.e. all residues C-terminal of the cyclizing

cysteine). All six of these displayed high affinity for ZIKVpro with dissociation constants (K_D) in the range of 5 – 168 nM as determined by surface plasmon resonance experiments (Table 1, Table S1, Figure S4). All of these compounds contain at least one unnatural modification in the peptide backbone and five out of six include the unnatural amino acid *N*-methyl-4-*O*-methyl-tyrosine ($^{Me}Y_{Me}$), suggesting that these features are crucial for high affinity.

The selected compounds were further analyzed with respect to their actual potential to inhibit the catalytic activity of the linked ZIKVpro construct (gZiPro) in a biochemical assay. All compounds except **5** showed significant inhibition of ZIKVpro substrate processing below a 100 μM cutoff (Table 1, Figure S5). Notably, **5** is the only analyzed peptide macrocycle that lacks the unnatural *O*-methyl-tyrosine side chain. Despite having no influence on catalytic activity, compound **5** binds to ZIKVpro with extraordinary affinity (K_D = 5 nM), indicating a tight binding event that is likely to be distant from the substrate binding site without any impact on the structural integrity of the catalytic center. Therefore, compound **5** linked to any reporter molecules (e.g. via a C-terminal amide bond) might have applications in selective probing of ZIKVpro without perturbing its activity. This exemplifies a major advantage of the presented affinity screening over conventional high-throughput screening methods for protease inhibitors, which usually focus on inhibition only.

Table 1. Affinity and inhibitory activity of macrocyclic peptides against flaviviral proteases.

Cpd.	Sequence[a]	ZIKV (gZiPro)[b]		ZIKV (bZiPro)[e]	DEN-Vpro[f]	WNVpro[g]
		K_i / μM[c] (IC_{50} / μM)	K_D / μM[d]	IC_{50} / μM[e]	IC_{50} / μM[f]	IC_{50} / μM[g]
1	-S-Ac-YWKI$^{Me}Y_{Me}$NTLVNIC-NH_2	0.80 ± 0.08 (1.32 ± 0.03)	0.02	1.5 ± 0.1	>10	>10
2	-S-Ac-Y$^{Me}Y_{Me}$K^{Me}FK^{Me}S$^{Me}Y_{Me}$K$^{Me}Y_{Me}{}^{Me}Y_{Me}$KC-NH_2	0.44 ± 0.03 (0.62 ± 0.04)	0.009	0.25 ± 0.01	1.7 ± 0.1	3.9 ± 0.4
3	-S-Ac-YTNFYLYPY$^{Me}Y_{Me}$FC-NH_2	2.0 ± 0.2 (3.3 ± 0.2)	0.008	2.2 ± 0.1	>20	>20
4	-S-Ac-Y^{Me}GIAKYN$^{Me}Y_{Me}{}^{Me}Y_{Me}$IPC-NH_2	20.4 ± 2.3 (16.5 ± 0.9)	0.009	4.6 ± 0.3	≥20	≥20
5	-S-Ac-YTLPFHN^{Me}GTFFC-NH_2	>100	0.005	≥50	>20	>20
6	-S-Ac-D-YAII$^{Me}Y_{Me}$YNKY^{Me}LNC-NH_2	3.5 ± 0.4 (7.1 ± 0.2)	0.168	3.2 ± 0.4	>20	>20

[a] The N-terminal thioether-acyl moiety (-S-Ac-) forms a macrocycle through the side chain of the underlined cysteine residue. $^{Me}Y_{Me}$, *N*-methyl-4-*O*-methyl-tyrosine; ^{Me}F, *N*-methyl-phenylalanine; ^{Me}S, *N*-methyl-serine; ^{Me}G, *N*-methyl-glycine; ^{Me}L, *N*-methyl-leucine; D-Y, D-tyrosine. [b] Zika virus NS2B-NS3 protease (linked construct) C80S/C143S (1 nM). Substrate: Bz-Nle-Arg-Lys-Lys-AMC. [c] Inhibition constants (K_i) were calculated from measurements at four different substrate concentrations using a non-competitive inhibition model (non-linear least-squares fits). Half maximal inhibitory concentrations (IC_{50}) for a substrate concentration of 15 μM are reported in parenthesis. [d] Dissociation constants (K_D) were determined by surface plasmon resonance using immobilized Zika virus NS2B-NS3 protease (gZiPro). [e] Zika virus NS2B-NS3 protease (unlinked construct; 0.5 nM). Substrate: Bz-Nle-Arg-Lys-Lys-AMC. Half maximal inhibitory concentrations (IC_{50}) were calculated for a substrate concentration of 15 μM. [f] Dengue virus serotype 2 NS2B-NS3 protease (100 nM). Substrate: Abz-Nle-Lys-Arg-Arg-Ser-3-(NO_2)Tyr. Half maximal inhibitory concentrations (IC_{50}) were calculated for a substrate concentration of 50 μM. [g] West Nile virus NS2B-NS3 protease (150 nM). Substrate: Abz-Gly-Leu-Lys-Arg-Gly-Gly-3-(NO_2)Tyr. Half maximal inhibitory concentrations (IC_{50}) were calculated for a substrate concentration of 50 μM.

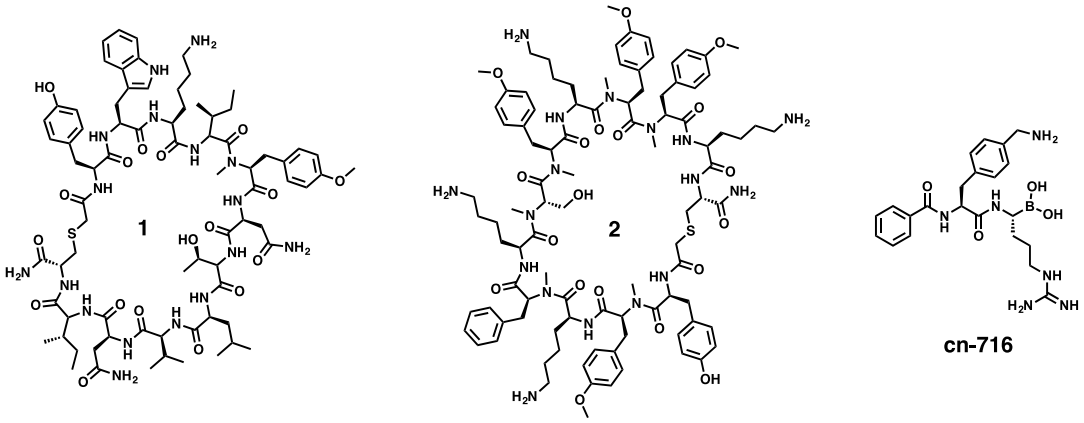

Figure 2. Chemical structures of synthesized hit compounds **1** and **2** that were identified as nanomolar non-competitive inhibitors of the Zika virus NS2B-NS3 protease. Compound **cn-716** is a previously published[4] covalent active-site inhibitor of the Zika virus NS2B-NS3 protease, which has been used in this study for comparison.

To exclude any construct-specific artifacts, we further assessed the activity of the unlinked ZIKVpro construct (bZiPro) in the presence of compounds **1-6** using the same biochemical assay. The IC_{50} values observed for gZiPro and bZiPro were mostly similar (Table 1, Figure S6), indicating that the linked (gZiPro) and unlinked (bZiPro) constructs are equally suitable templates for drug discovery campaigns. Compounds **1** and **2** displayed the strongest inhibition of ZIKVpro with inhibition constants firmly in the nanomolar range (Table 1). These two macrocyclic peptides are structurally unrelated (Figure 2) and may therefore serve as independent starting points for further optimizations. In contrast to the previously reported ZIKVpro active-site inhibitor **cn-716**, which showed strong inhibition of thrombin (IC_{50} = 0.5 μM) and trypsin (IC_{50} = 0.05 μM),[8] neither compound **1** nor **2** displayed thrombin or trypsin inhibition at the highest assayed concentrations of 25 μM and 50 μM, respectively (data not shown), highlighting their specificity towards ZIKVpro.

Mechanistic studies with gZiPro at various substrate and inhibitor concentrations revealed a non-competitive inhibition mode for compounds **1–4** and **6**, as evidenced both by non-linear least-squares data fits (Table S3) and Cornish-Bowden plots. As an example, Figure 3A shows the Cornish-Bowden plot for the most active peptide **2**, where the abscissa intersection point clearly indicates non-competitive binding.[22] As expected for the non-competitive binding model, the degree of inhibition was independent of the substrate concentration, even at multiples of the K_m value. Due to the size of substrate and macrocyclic inhibitor, both cannot occupy the active site simultaneously, suggesting that compounds **1–4** and **6** may act as allosteric antagonists of ZIKVpro activity. Allosteric inhibitors have been reported previously for dengue virus NS2B-NS3 proteases at different sites of NS3,[23, 24] which may also act by perturbing the essential interactions between NS2B and NS3.[25] As expected for allosteric inhibitors, the K_i values were all greater than the K_D values, suggesting inhibition by locking the protease in conformations less competent for catalysis (in the most extreme case, compound **5** binds with high affinity but does not affect the catalytic rate at all).

Figure 3. A: Cornish-Bowden plot for compound **2** and Zika virus NS2B-NS3 protease (gZiPro). The intersection point (–K_i) of the four independent linear fits with the abscissa indicates a non-competitive inhibition mechanism with a K_i value of 0.44 μM.[22] The same value was obtained from non-linear least-squares fits using a non-competitive binding model (Graphpad Prism 7.0; Table S3). **B**: Inhibition of Zika virus NS2B-NS3 protease (bZiPro) activity by the non-competitive inhibitor **2** and the covalently binding active-site inhibitor **cn-716**. Addition of compound **2** in the presence of **cn-716** results

in synergistically decreased protease activity, suggesting that **2** binds at an allosteric site.

Although, in principle, resistance may easily evolve against allosteric inhibitors of viral proteases, such inhibitors can be valuable therapeutics in combination with substrate-derived active-site inhibitors. Established reverse transcriptase inhibitors for the treatment of chronic HIV infections are a prominent example.[26] As drug-like active-site inhibitors of flaviviral proteases suffer from low affinity, their combination with allosteric antagonists is a promising route toward anti-flaviviral therapeutics with adequate pharmacokinetic properties. To support the potential allosteric binding mode indicated by the non-competitive inhibition data, we performed the activity assay with bZiPro in the presence and absence of compound **2** and the covalent active-site inhibitor **cn-716** (Figure 3B). As expected, the simultaneous presence of inhibitor **2** and **cn-716** inhibited the ZIKVpro activity more strongly than the individual compounds at identical concentrations, indicating synergistic inhibition of ZIKVpro (Figure 3B). As **cn-716** is known to occupy the active site by binding covalently to the active-site serine residue 135,[4] this is strong evidence for compound **2** binding to a site distant from the substrate-binding site. Unfortunately, attempts to verify the allosteric binding mode by NMR spectroscopy or X-ray crystallography have failed to date because of the low solubility of the inhibitors.

To further assess the specificity of the discovered inhibitors, we tested their performance with dengue and West Nile virus proteases (Table 1). Only compound **2** showed significant inhibition of both proteases in the low micromolar range with selectivity indices of 4 and 9 in favor of ZIKVpro over the dengue and West Nile virus proteases, respectively. Compounds **1** and **3** displayed selectivity indices greater than 10 in favor of ZIKVpro. Only compound **4** showed similarly weak inhibition constants around 20 μM for all three viral proteases. The selectivity of our new inhibitors toward ZIKVpro is in stark contrast to the broad cross-reactivity of previously described flaviviral protease inhibitors, which are predominantly active-site inhibitors.[7] As the active center is highly conserved, selective targeting has been difficult in the past. Consequently, several compounds that were previously discovered as inhibitors of dengue and West Nile virus proteases have also been reported to inhibit ZIKVpro or even human serine proteases.[7] The completely new structural motifs of the present study thus not only allow an increase in inhibition by non-competitive interactions but also selective probing of ZIKVpro.

The most active compound **2** (K_i = 0.44 μM, K_D = 0.009 μM; gZiPro) exhibits multiple non-canonical structural features. Half of all backbone nitrogen atoms of peptide **2** are methylated and it contains four unnatural *O*-methyltyrosine side chains, representing a chemical complexity that would require several optimization cycles underpinned by successful structure-activity relationships if starting from a canonical peptide library. None of the selected screening hits showed evidence for competitive inhibition at the active site of the protease. This bias toward the enrichment of sequences that may target exosites rather than the active site of ZIKVpro suggests that active-site interactions of macrocycles were of significantly lower affinity during the screening (preventing enrichment of those sequences). This in turn suggests low druggability of the active site of ZIKVpro (and closely related flaviviruses) by classical competitive inhibitors. This conclusion is supported by a previous study that aimed to identify high-affinity active site inhibitors in a library of substrate analogues, where interactions with key residues in the active site could be established but only an additional covalent bond with the catalytic serine residue yielded affinities in the nanomolar range (as in **cn-716**, Figure 2).[4, 8] Alternatively, the absence of competitive inhibitors in the present work may be related to the deliberate exclusion of arginine (to avoid pharmacokinetic liabilities). All flaviviral proteases share the recognition of basic residues (arginine and lysine) in the non-prime substrate site with a particular preference for arginine in P_1 and most peptide-based inhibitors address this recognition motif.[3, 8, 9, 27-30] By excluding arginine from our screening library, we not only avoided an amino acid with a potentially negative impact on drug-likeness, but apparently also favored the selection of non-competitive inhibitors.

Figure 4. Effect of compounds **1** and **2** on the metabolic activity of Huh-7 cells (% reduction compared to non-treated). The dotted lines indicate an 80% cell-viability cut-off. Neither compound shows significant cytotoxic effects at concentrations up to 12.5 μM. **A**: 24 h incubation. **B**: 48 h incubation.

The two most active compounds from this screening campaign, **1** and **2**, displayed no cytotoxic effects at concentrations up to 12.5 μM after 24 and 48 hours of incubation with Huh-7 cells (Figure 4). At higher concentrations cytotoxic effects became apparent only for compound **2**. This result underlines the potential of the macrocyclic peptides **1** and **2** as ZIKVpro lead compounds, as they combine nanomolar dissociation and inhibition constants with unusual (non-competitive) inhibition mechanisms, excellent selectivity against human proteases, and low cytotoxicity. Our study also demonstrates that display screenings offer an excellent way to rapidly generate selective probes and tool compounds that can modulate the enzymatic activity of the target protein from fully active (**5**) to highly inhibited (**2**). Future attempts will focus on further derivatizations of the identified and validated hits **1** and **2** to allow deeper insights into structure-activity relationships and facilitate in-cell studies and the generation of structural data by X-ray crystallography and NMR spectroscopy. These studies will capitalize on chemical opportunities provided by the exocyclic C-termini of these compounds that can readily be tagged with reporter molecules or moieties that modulate solubility or cellular uptake without altering the macrocyclic peptide structure.

In conclusion, we present the first macrocyclic peptide inhibitors of ZIKVpro identified through a RaPID screening technique that is orthogonal to conventional high-throughput approaches. With a single selection screen and no further optimizations, we identified unnatural peptides of remarkable affinity, inhibitory activity, and target selectivity. Most importantly, our results indicate that non-competitive inhibitors can be made that are highly active and may present excellent options for probes, tools and potential drug candidates in comparison to active-site inhibitors that have been unsuccessfully pursued for a very long time. Future work will assess whether a combination of competitive and non-competitive inhibitors indeed offers a superior approach for the development of antiviral agents against Zika, dengue and related viral infectious diseases.

ASSOCIATED CONTENT

Supporting Information

The Supporting Information is available free of charge on the ACS Publications website.

Experimental details for Zika, dengue and West Nile virus protease constructs and preparation, synthesis and screening of macrocyclic peptide library, solid phase peptide synthesis, surface plasmon resonance, enzymatic protease assays (Zika, dengue, West Nile, thrombin, trypsin), cellular assays. Figure S1 (RaPID screening process), Figure S2 (alignment of peptide sequences), Figure S3 (MS data), Figure S4 (SPR binding curves), Figures S5 and S6 (dose-response curves), Figure S7 (Huh-7 cell viability data), Table S1 (SPR kinetic parameters), Table S2 (DNA oligonucleotide sequences), Table S3 (non-linear least-squares fitting parameters).

AUTHOR INFORMATION

Corresponding Authors

* E-mail: christoph.nitsche@anu.edu.au
hsuga@chem.s.u-tokyo.ac.jp

Author Contributions

# These authors contributed equally. All authors have given approval to the final version of the manuscript.

ORCID

Christoph Nitsche: 0000-0002-3704-2699
Toby Passioura: 0000-0002-6089-5067
Mithun C. Mahawaththa: 0000-0001-5171-6744
Mila M. Leuthold: 0000-0001-7698-2360
Christian D. Klein: 0000-0003-3522-9182
Hiroaki Suga: 0000-0002-5298-9186
Gottfried Otting: 0000-0002-0563-0146

ACKNOWLEDGMENT

C.N. thanks the Alexander von Humboldt Foundation for a Feodor Lynen Research Fellowship. Financial support by the Australian Research Council, including a Laureate Fellowship for G.O. is gratefully acknowledged. This work was also partially supported by CREST for Molecular Technologies, JST, and JSPS KAKENHI (16H06444 and 26220204) to H.S. We thank Mrs. Natascha Stefan for technical support.

REFERENCES

1. Baud, D.; Gubler, D. J.; Schaub, B.; Lanteri, M. C.; Musso, D. An update on Zika virus infection. *Lancet* **2017,** *390*, 2099–2109.
2. Poland, G. A.; Kennedy, R. B.; Ovsyannikova, I. G.; Palacios, R.; Ho, P. L.; Kalil, J. Development of vaccines against Zika virus. *Lancet Infect. Dis.* **2018,** *18*, e211–e219.
3. Nitsche, C.; Holloway, S.; Schirmeister, T.; Klein, C. D. Biochemistry and medicinal chemistry of the dengue virus protease. *Chem. Rev.* **2014,** *114*, 11348–11381.
4. Lei, J.; Hansen, G.; Nitsche, C.; Klein, C. D.; Zhang, L.; Hilgenfeld, R. Crystal structure of Zika virus NS2B-NS3 protease in complex with a boronate inhibitor. *Science* **2016,** *353*, 503–505.
5. Zhang, Z.; Li, Y.; Loh, Y. R.; Phoo, W. W.; Hung, A. W.; Kang, C.; Luo, D. Crystal structure of unlinked NS2B-NS3 protease from Zika virus. *Science* **2016,** *354*, 1597–1600.
6. Phoo, W. W.; Li, Y.; Zhang, Z.; Lee, M. Y.; Loh, Y. R.; Tan, Y. B.; Ng, E. Y.; Lescar, J.; Kang, C.; Luo, D. Structure of the NS2B-NS3 protease from Zika virus after self-cleavage. *Nat. Commun.* **2016,** *7*, 13410.
7. Nitsche, C. Strategies towards protease inhibitors for emerging flaviviruses. In *Dengue and Zika: Control and Antiviral Treatment Strategies*, Hilgenfeld, R.; Vasudevan, S. G., Eds. Springer: Singapore, 2018; pp 175–186.
8. Nitsche, C.; Zhang, L.; Weigel, L. F.; Schilz, J.; Graf, D.; Bartenschlager, R.; Hilgenfeld, R.; Klein, C. D. Peptide–boronic acid inhibitors of flaviviral proteases: medicinal chemistry and structural biology. *J. Med. Chem.* **2017,** *60*, 511–516.
9. Li, Y.; Zhang, Z.; Phoo, W. W.; Loh, Y. R.; Wang, W.; Liu, S.; Chen, M. W.; Hung, A. W.; Keller, T. H.; Luo, D.; Kang, C. Structural dynamics of Zika virus NS2B-NS3 protease binding to dipeptide inhibitors. *Structure* **2017,** *25*, 1242–1250.
10. Roy, A.; Lim, L.; Srivastava, S.; Lu, Y.; Song, J. Solution conformations of Zika NS2B-NS3pro and its inhibition by natural products from edible plants. *PLoS One* **2017,** *12*, e0180632.
11. Shiryaev, S. A.; Farhy, C.; Pinto, A.; Huang, C. T.; Simonetti, N.; Elong Ngono, A.; Dewing, A.; Shresta, S.; Pinkerton, A. B.; Cieplak, P.; Strongin, A. Y.; Terskikh, A. V. Characterization of

the Zika virus two-component NS2B-NS3 protease and structure-assisted identification of allosteric small-molecule antagonists. *Antiviral Res.* **2017,** *143*, 218–229.

12. Passioura, T.; Katoh, T.; Goto, Y.; Suga, H. Selection-based discovery of druglike macrocyclic peptides. *Annu. Rev. Biochem.* **2014,** *83*, 727–752.

13. Passioura, T.; Watashi, K.; Fukano, K.; Shimura, S.; Saso, W.; Morishita, R.; Ogasawara, Y.; Tanaka, Y.; Mizokami, M.; Sureau, C.; Suga, H.; Wakita, T. *De novo* macrocyclic peptide inhibitors of hepatitis B virus cellular entry. *Cell Chem. Biol.* **2018,** *25*, 906–915.

14. Yamagishi, Y.; Shoji, I.; Miyagawa, S.; Kawakami, T.; Katoh, T.; Goto, Y.; Suga, H. Natural product-like macrocyclic N-methyl-peptide inhibitors against a ubiquitin ligase uncovered from a ribosome-expressed *de novo* library. *Chem. Biol.* **2011,** *18*, 1562–1570.

15. Goto, Y.; Ohta, A.; Sako, Y.; Yamagishi, Y.; Murakami, H.; Suga, H. Reprogramming the translation initiation for the synthesis of physiologically stable cyclic peptides. *ACS Chem. Biol.* **2008,** *3*, 120–129.

16. Song, X.; Lu, L. Y.; Passioura, T.; Suga, H. Macrocyclic peptide inhibitors for the protein-protein interaction of Zaire Ebola virus protein 24 and karyopherin alpha 5. *Org. Biomol. Chem.* **2017,** *15*, 5155–5160.

17. Jongkees, S. A. K.; Caner, S.; Tysoe, C.; Brayer, G. D.; Withers, S. G.; Suga, H. Rapid discovery of potent and selective glycosidase-inhibiting *de novo* peptides. *Cell Chem. Biol.* **2017,** *24*, 381–390.

18. Matsunaga, Y.; Bashiruddin, N. K.; Kitago, Y.; Takagi, J.; Suga, H. Allosteric inhibition of a semaphorin 4D receptor plexin B1 by a high-affinity macrocyclic peptide. *Cell Chem. Biol.* **2016,** *23*, 1341–1350.

19. Hacker, D. E.; Hoinka, J.; Iqbal, E. S.; Przytycka, T. M.; Hartman, M. C. Highly constrained bicyclic scaffolds for the discovery of protease-stable peptides via mRNA display. *ACS Chem. Biol.* **2017,** *12*, 795–804.

20. Kale, S. S.; Villequey, C.; Kong, X. D.; Zorzi, A.; Deyle, K.; Heinis, C. Cyclization of peptides with two chemical bridges affords large scaffold diversities. *Nat. Chem.* **2018,** *10*, 715–723.

21. Rentero Rebollo, I.; McCallin, S.; Bertoldo, D.; Entenza, J. M.; Moreillon, P.; Heinis, C. Development of potent and selective *S. aureus* sortase A inhibitors based on peptide macrocycles. *ACS Med. Chem. Lett.* **2016,** *7*, 606–611.

22. Cornish-Bowden, A. A simple graphical method for determining the inhibition constants of mixed, uncompetitive and non-competitive inhibitors. *Biochem. J.* **1974,** *137*, 143–144.

23. Yildiz, M.; Ghosh, S.; Bell, J. A.; Sherman, W.; Hardy, J. A. Allosteric inhibition of the NS2B-NS3 protease from dengue virus. *ACS Chem. Biol.* **2013,** *8*, 2744–2752.

24. Wu, H.; Bock, S.; Snitko, M.; Berger, T.; Weidner, T.; Holloway, S.; Kanitz, M.; Diederich, W. E.; Steuber, H.; Walter, C.; Hofmann, D.; Weissbrich, B.; Spannaus, R.; Acosta, E. G.; Bartenschlager, R.; Engels, B.; Schirmeister, T.; Bodem, J. Novel dengue virus NS2B/NS3 protease inhibitors. *Antimicrob. Agents Chemother.* **2015,** *59*, 1100–1109.

25. Brecher, M.; Li, Z.; Liu, B.; Zhang, J.; Koetzner, C. A.; Alifarag, A.; Jones, S. A.; Lin, Q.; Kramer, L. D.; Li, H. A conformational switch high-throughput screening assay and allosteric inhibition of the flavivirus NS2B-NS3 protease. *PLoS Pathog.* **2017,** *13*, e1006411.

26. De Clercq, E. The design of drugs for HIV and HCV. *Nat. Rev. Drug. Discov.* **2007,** *6*, 1001–1018.

27. Phoo, W. W.; Zhang, Z.; Wirawan, M.; Chew, E. J. C.; Chew, A. B. L.; Kouretova, J.; Steinmetzer, T.; Luo, D. Structures of Zika virus NS2B-NS3 protease in complex with peptidomimetic inhibitors. *Antiviral Res.* **2018,** *160*, 17–24.

28. Nitsche, C.; Behnam, M. A.; Steuer, C.; Klein, C. D. Retro peptide-hybrids as selective inhibitors of the dengue virus NS2B-NS3 protease. *Antiviral Res.* **2012,** *94*, 72–79.

29. Nitsche, C.; Schreier, V. N.; Behnam, M. A.; Kumar, A.; Bartenschlager, R.; Klein, C. D. Thiazolidinone-peptide hybrids as dengue virus protease inhibitors with antiviral activity in cell culture. *J. Med. Chem.* **2013,** *56*, 8389–8403.

30. Weigel, L. F.; Nitsche, C.; Graf, D.; Bartenschlager, R.; Klein, C. D. Phenylalanine and phenylglycine analogues as arginine mimetics in dengue protease inhibitors. *J. Med. Chem.* **2015,** *58*, 7719–7733.

Supporting Information

De Novo Discovery of Nonstandard Macrocyclic Peptides as Non-Competitive Inhibitors of the Zika Virus NS2B-NS3 Protease

Christoph Nitsche, Toby Passioura, Paul Varava, Mithun C. Mahawaththa, Mila M. Leuthold, Christian D. Klein, Hiroaki Suga, and Gottfried Otting

Preparation of linked Zika virus NS2B-NS3 protease (gZiPro). The construct has been described previously.[1, 2] Briefly, it includes 48 hydrophilic core residues of NS2B followed by a GGGGSGGGG linker, the 170 N-terminal residues of the NS3 protease domain and a C-terminal His_6 tag. The mutations C80S and C143S were introduced to avoid dimerization by oxidation. The T7 expression vector pETMCSI[3] was transformed into *E. coli* BL21(DE3) cells, which were grown in LB medium at 37 °C until an OD_{600} value of 0.6 was reached. Subsequently, overexpression was induced with IPTG (1 mM), and the cells were incubated at room temperature overnight. The cells were pelleted by centrifuging at 5,000 *g* for 10 minutes and lysed by passing through a French Press (SLM Aminco) at 830 bars. The cell lysate was centrifuged for 1 h at 34,000 *g* and the supernatant was loaded onto a 5 mL Co-NTA column (GE Healthcare Life Science) pre-equilibrated with buffer A (50 mM Tris-HCl, pH 7.5, 300 mM NaCl, 10% (v/v) glycerol). The protein was eluted with a linear gradient of buffer A supplemented with 300 mM imidazole, fractions were analyzed by 12% SDS-PAGE, and the buffer was exchanged to 50 mM phosphate, pH 7.0, and 50 mM NaCl.

Preparation of unlinked Zika virus NS2B-NS3 protease (bZiPro). The construct was obtained from Addgene (plasmid #86846) and expressed and purified exactly as described previously.[4]

Synthesis and screening of peptide library. Library construction and screening were performed essentially as described previously (Figure S1).[5-11] Briefly, DNA templates for the construction of mRNA libraries were synthesized by primer extension and PCR using the primers shown in Table S2. Cognate mRNAs were generated by T7 polymerase-mediated transcription and covalently linked to PEG-puromycin, before translation in reprogrammed *in vitro* translation reactions without Asp, Glu, Met, and Arg and their cognate aminoacyl-tRNA synthetases, as previously described.[12] Each reaction contained 1.2 μM mRNA-puro, 12.5 μM initiator tRNA ($tRNA^{fMet}$ aminoacylated with ClAc-Tyr), and 25 μM of each elongator tRNA (an engineered Glu tRNA including an anticodon of choice - EnGluxxx, see Table S2) aminoacylated with the specified non-canonical amino acid. In the first round of selection, translation was performed at 150 μL scale to produce approximately $1.2 \cdot 10^{14}$ molecules. After translation, peptide-mRNA conjugates were isolated from the ribosomes by EDTA treatment and reverse transcribed using the CGT3an13.R23 primer and RNase H-reverse transcriptase

(Promega). Peptide-mRNA conjugate libraries were panned against 200 nM C-terminally His_6-tagged linked Zika virus NS2B-NS3 protease (gZiPro) immobilized on Dynabeads™ (His-tag isolation and pulldown - Thermo Fisher) at 4 °C for 30 min, the beads were washed three times with cold PBS-T (10 mM phosphate, pH 7.4, 130 mM NaCl, 0.05% (v/v) Tween-20), and cDNA was recovered by PCR using the primers T7g10m.F46 and CGT3an13.R23 prior to T7 transcription to generate the mRNA for a second round of selection. In the second and later rounds of selection, translation was performed at 5 μL scale and libraries were subjected to 6 rounds of counter selection against uncoated beads prior to panning against linked Zika virus NS2B-NS3 protease (gZiPro). Assessment of recovery following each round was performed by quantitative real time PCR using Sybr Green I dye (Lonza Japan Ltd) on a light cycler nanothermal cycler (Roche). DNA from each round was sequenced using a MiSeq high-throughput sequencer (Illumina) and analyzed using CLC workbench software (Qiagen) as previously described.[9] Following alignment of the 100 most enriched sequences (Figure S2), peptide families were defined as groups of close analogues for which at least 2 sequences were identified, and the most abundant peptide from each was chosen for solid phase synthesis and further characterisation.

Solid phase peptide synthesis. Macrocyclic peptides were synthesized at 25 μmol scale using standard Fmoc solid phase peptide synthesis methodology using HBTU, HOBt, diisopropylethylamine (DIPEA), Rink amide resin, and a Syro I automated synthesizer (Biotage). All amino acids and coupling reagents were purchased from Watanabe Chemical Ltd, except for DIPEA (Wako Japan). For synthesis of *N*-methyl-*O*-methyl-tyrosine residues, *O*-methyl-tyrosine coupling was followed by Fmoc deprotection, nosyl protection of the resulting free amine, and on-resin methylation using dimethyl sulfate as follows: following Fmoc deprotection, 2-nitrobenzenesulfonyl chloride (22 mg, 0.1 mmol) in *N*-methyl-2-pyrrolidone (NMP) and 2,4,6-trimethylpyridine (33 μL, 0.25 mmol) were added to the resin, the reaction was allowed to proceed for 15 min at room temperature, and the resin was washed (five times) with NMP. Methylation was performed twice using 1,8-diazabicyclo(5.4.0)undec-7-ene (11.25 μL, 0.075 mmol) and dimethyl sulfate (22.25 μL, 0.25 mmol) in NMP for 5 minutes, after which the resin was washed (five times) with NMP. Nosyl deprotection was performed twice using 1,8-diazabicyclo(5.4.0)undec-7-ene (18.75 μL, 0.125 mmol) and 2-mercaptoethanol (17.5 μL, 0.25 mmol) in NMP for 5 minutes, after which the resin was washed

(five times) with NMP and solid phase peptide synthesis was continued. Identity and purity of all peptides were confirmed by MALDI-TOF MS (Figure S3).

Zika virus NS2B-NS3 protease enzymatic inhibition assay. All measurements were performed in triplicate in 10 mM Tris-HCl, pH 8.5, 20% (v/v) glycerol, and 1 mM CHAPS as described previously.[13, 14] Different concentrations (ranging from 0 to 100 μM) of compounds **1**-**6** (10 mM DMSO stocks) were pipetted into a 96-well plate (black U-bottom, Greiner, Bio-One). Zika virus NS2B-NS3 protease was added to a final concentration of 1 nM (gZiPro) or 0.5 nM (bZiPro) and the mixture was incubated for 10 min. Subsequently, the enzymatic reaction was initiated by adding the substrate Bz-Nle-Lys-Lys-Arg-AMC (Biosyntan) to four final concentrations (15, 30, 45, 60 μM). The gradual release of fluorescent 7-amino-4-methylcoumarin (AMC) was monitored for 3 min at 460 nm with excitation at 360 nm, using a fluorophotometer (Spectramax M2e plate reader, Molecular Devices). Initial velocities were derived from the linear curves as variation of relative fluorescence intensity per unit time. The relative fluorescence units were converted to the amount of cleaved substrate via a calibration curve as described previously.[14] IC_{50} values were calculated from at least seven different inhibitor concentrations using Prism 7.0 (Graphpad Software). K_i values for a non-competitive inhibition model were calculated using Prism 7.0 (GraphPad Software) using non-linear least-squares fits.

Surface plasmon resonance (SPR) determination of binding kinetics. Binding kinetics of each macrocyclic peptide toward Zika virus NS2B-NS3 protease were determined using a Biacore T200 SPR instrument (GE Healthcare Life Sciences). Target protein was immobilized on a CM5 chip using EDC/NHS chemistry (Amine Coupling Kit, GE Healthcare Life Sciences) to a signal level of ~2000 RU. Binding kinetics were assessed by injection of varying concentrations of compounds **1**-**6** dissolved in 10 mM HEPES, pH 7.4, 150 mM NaCl, 0.5% (v/v) polysorbate 20, 0.1% (v/v) DMSO with target regeneration using 10 mM glycine buffer, pH 1.5.

Preparation of dengue and West Nile virus NS2B-NS3 proteases. The protease constructs of dengue serotype 2 and West Nile virus were described previously.[15, 16] In both constructs the core sequence of NS2B is covalently ligated to the protease NS3 domain by a GGGGSGGGG

linker. Transformation of the pET28a plasmids (Novagen), expression of the His_6-tagged proteins in *E. coli* BL21(DE3) cells, and purification by nickel affinity chromatography were performed following a previously described protocol.[15, 16]

Dengue and West Nile virus NS2B-NS3 protease enzymatic inhibition assays. All measurements were performed in triplicate as described previously.[15, 16] Briefly, continuous assays were performed in 50 mM Tris-HCl, pH 9, 10% (v/v) ethylene glycol, and 0.0016% Brij 58 using a BMG Labtech Fluostar OPTIMA microtiter fluorescence plate reader and black 96 well V-bottom plates (Greiner Bio-One, Germany) with an excitation wavelength of 320 nm and a monitored emission wavelength of 405 nm. Compounds **1**-**6** (10 mM in DMSO) were incubated with the dengue virus protease (100 nM) or West Nile virus protease (150 nM) for 15 min before the enzymatic reaction was initiated by addition of the FRET substrates (final concentration 50 µM) Abz-Nle-Lys-Arg-Arg-Ser-3-(NO_2)Tyr (dengue virus protease) or Abz-Gly-Leu-Lys-Arg-Gly-Gly-3-(NO_2)Tyr (West Nile virus protease). The enzymatic activity was monitored for 15 min and initial velocities were derived from the linear curves as variation of relative fluorescence intensity per unit time. IC_{50} values were calculated from at least seven different inhibitor concentrations using Prism 7.0 (Graphpad Software).

Thrombin and trypsin enzymatic assays. All measurements were performed in triplicate as described previously.[16] Briefly, black 96 well V-bottom plates (Greiner Bio-One), a BMG Labtech Fluostar OPTIMA microtiter fluorescence plate reader operating at an excitation wavelength of 355 nm and an emission wavelength of 460 nm, and a buffer consisting of 50 mM Tris-HCl pH 7.5, 150 mM NaCl, and 0.05% Tween 20 were used. Compounds **1** and **2** were preincubated with thrombin (10 nM) or trypsin (1 nM) for 15 minutes at final concentrations of 25 and 50 µM, respectively. The cleavage reaction was initiated by addition of the Boc-Val-Pro-Arg-AMC substrate (Bachem, Switzerland) at a final concentration of 50 µM. The activities of thrombin and trypsin were determined as fluorescence increase (RFU/s) and monitored for 10 min.

Huh-7 metabolic activity assay. Huh-7 cells were seeded into 96-well cell culture plates at a density of 10^4 cells per well in a final volume of 100 µl. Treatment with compounds **1** and **2** was performed immediately after seeding at a starting concentration of 50 µM and a 2-fold serial dilution. After incubation for 24 h or 48h at 37 °C, the medium was replaced by fresh

DMEM and cell viability was measured by adding 20 µl per well CellTiter-Blue® reagent (Promega), which monitors the metabolic conversion of resazurin (λ_{max} = 605 nm) to resorufin (λ_{max} = 573 nm). Subsequently, cells were incubated for 1 h at 37 °C and the absorbance was measured at 600 and 570 nm. For evaluation the difference in absorbance values (absolute values or relative to the non-treated control) were plotted against the compound concentration.

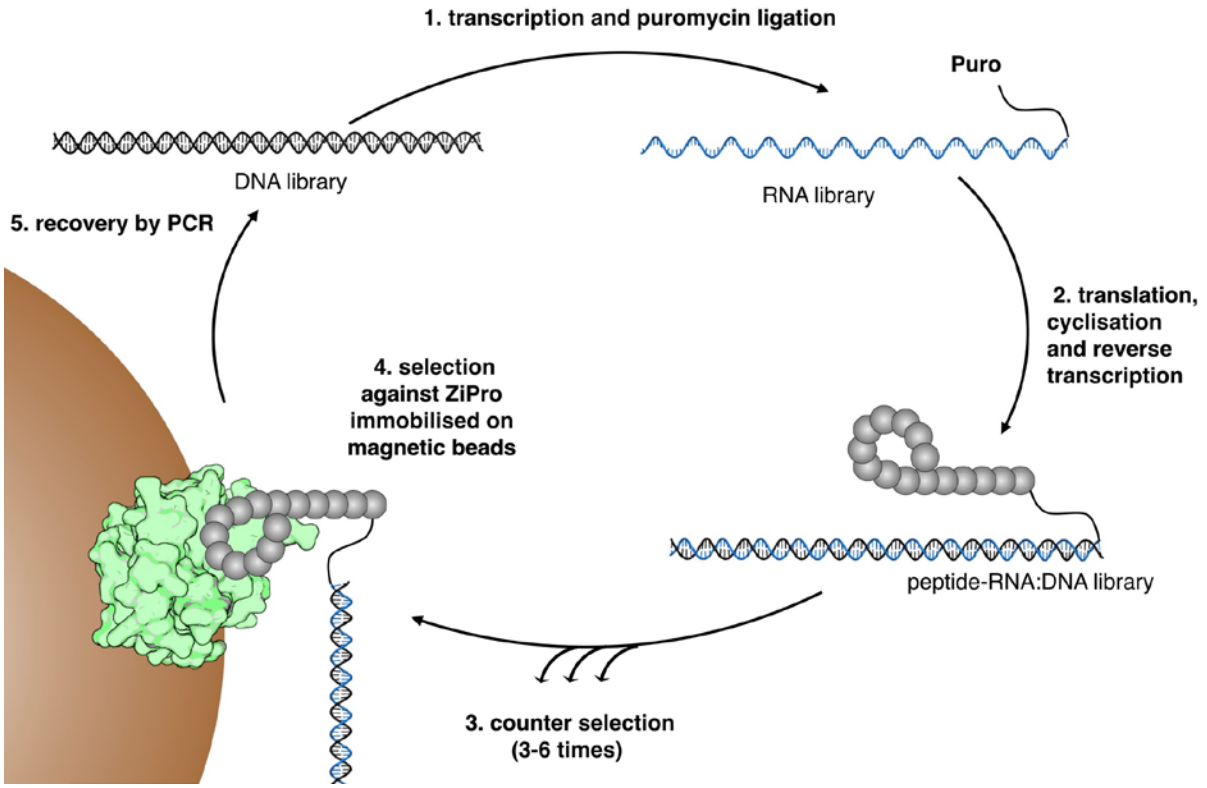

Figure S1. Schematic illustration of RaPID screening process. 1. A DNA library assembled from synthetic oligonucleotides is transcribed into RNA (blue) and ligated to puromycin at the 3' end. 2. This library is translated in a genetically reprogrammed reaction, resulting in a macrocyclic peptide library in which each peptide is covalently linked to its cognate mRNA. This is then reverse transcribed to generate peptide-RNA:DNA molecules. 3. Counter selections are used to remove peptides that bind non-specifically to the bead surface. 4. The library is then panned against Zika virus NS2B-NS3 protease immobilised on magnetic beads. 5. An enriched DNA library is then recovered by PCR and the process is repeated until increased rates of target binding are observed. Deconvolution of the library can be achieved through sequencing of the final (and intermediate) enriched DNA libraries.

Figure S2. Alignment of peptide sequences identified following selection for Zika virus NS2B-NS3 ligands. The hundred most frequent peptides from each library are shown. Sequences from the ClAc-L-tyrosine initiated library are shown in the left-hand column, and sequences from the ClAc-D-tyrosine initiated library are shown in the right-hand column. Other non-canonical amino acids are represented as indicated in the legend. Percentage values next to each sequence indicate overall prevalence in the enriched library. Black brackets show the breakdown of the identified sequences into 6 families (5 ClAc-L-tyrosine initiated and 1 ClAc-D-tyrosine initiated). Red arrows indicate sequences chosen for synthesis and further characterization, with numbers corresponding to the compounds listed in Table 1.

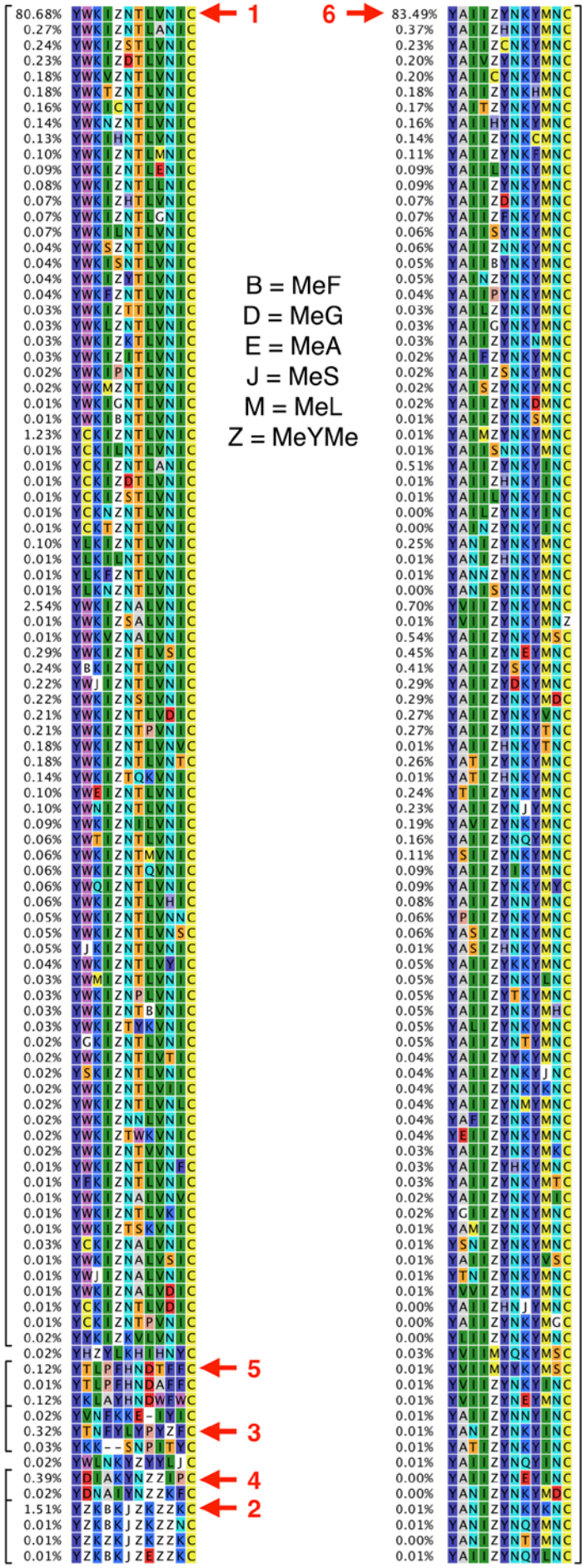

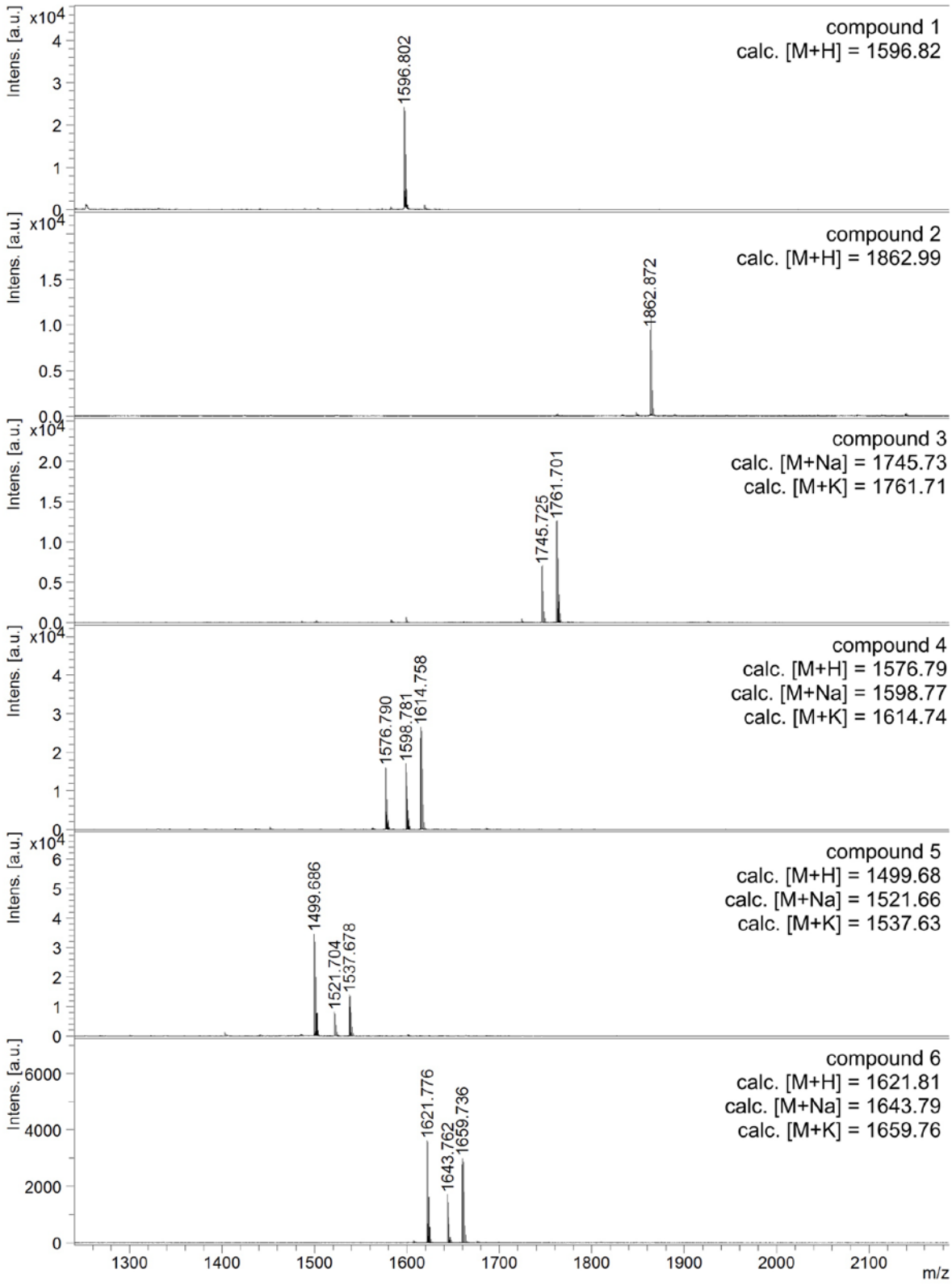

Figure S3. MALDI-TOF MS analysis of synthesized peptides.

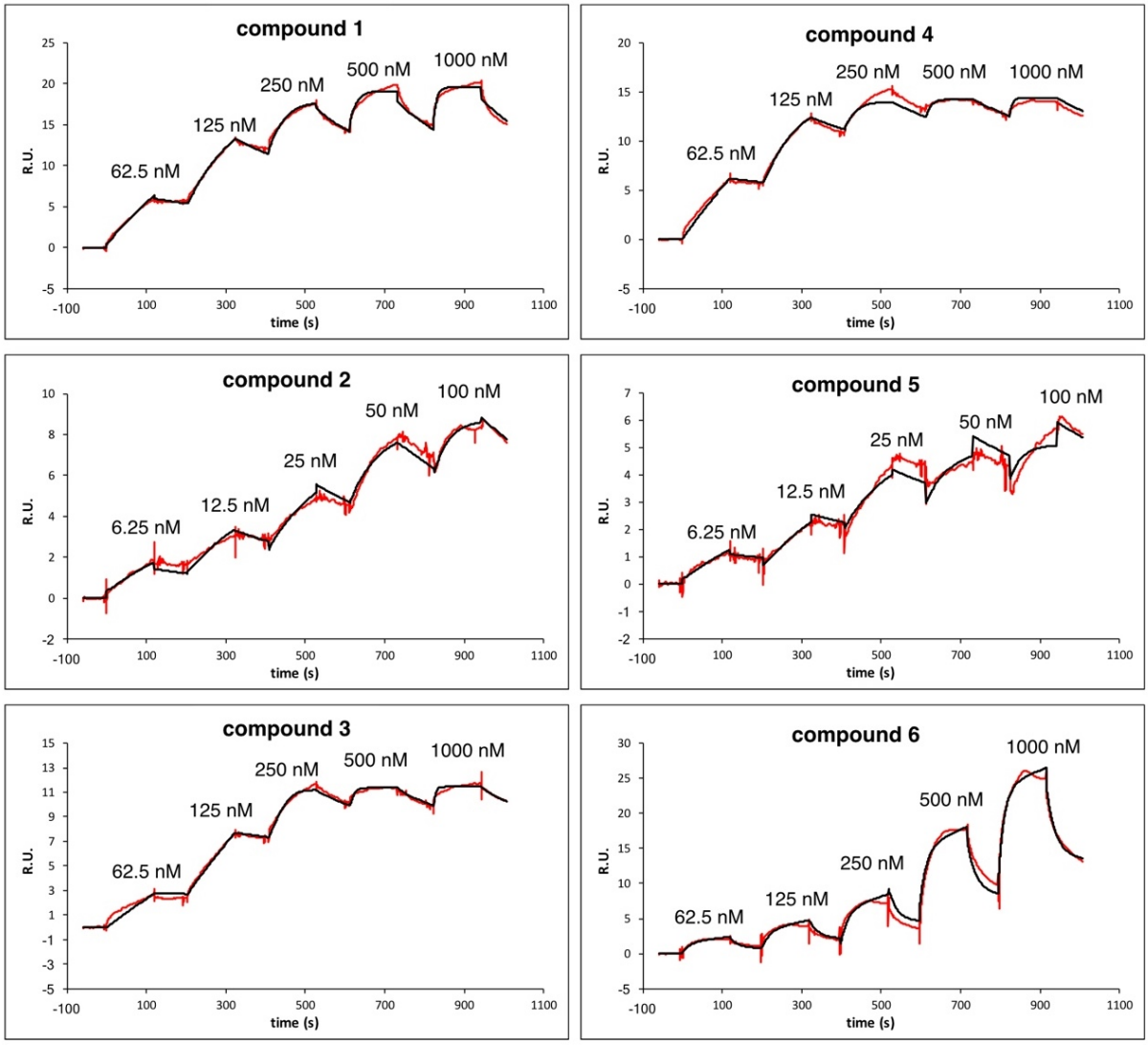

Figure S4. Zika virus NS2B-NS3 protease binding kinetics of compounds 1-6. Single-cycle kinetics experiments were performed using surface immobilized Zika virus NS2B-NS3 protease (gZiPro) with varying concentrations of macrocyclic peptide analyte. Compounds were analysed at the concentrations indicated. Kinetic parameters (see Table S1) were determined by fitting a 1:1 binding model, with the exception of compound **6** which was fitted using a two-state binding model. In each case, the red line indicates the data trace, and the black line indicates the fitted curve.

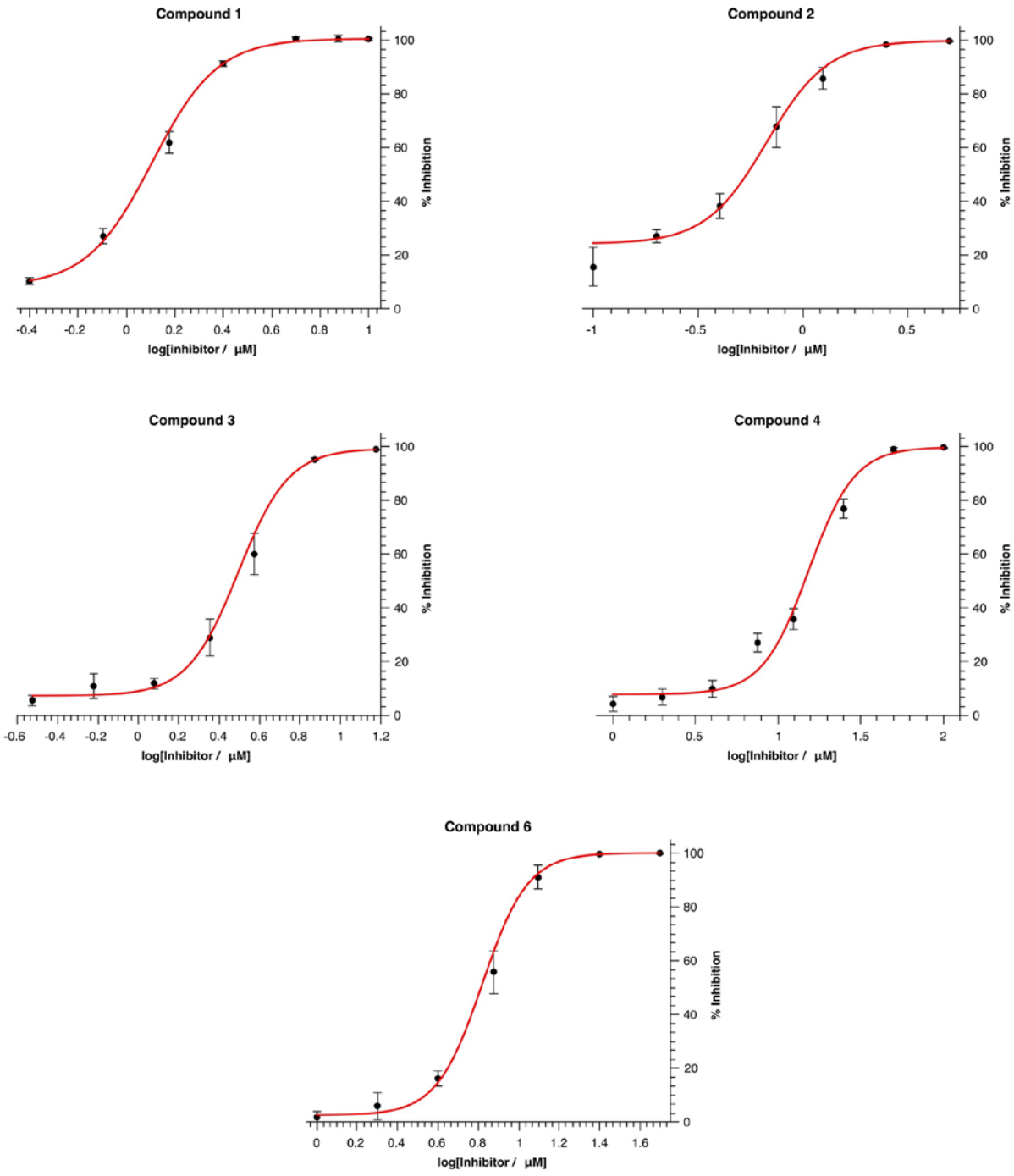

Figure S5. Dose response curves of Zika virus NS2B-NS3 protease inhibitors. Measurements were performed in triplicate at concentrations of 15 µM substrate and 1 nM linked Zika virus NS2B-NS3 protease (gZiPro). Dose-response curves were fitted using a sigmoid fitting function. Similar dose-response curves were recorded for at least three additional substrate concentrations to derive K_i values.

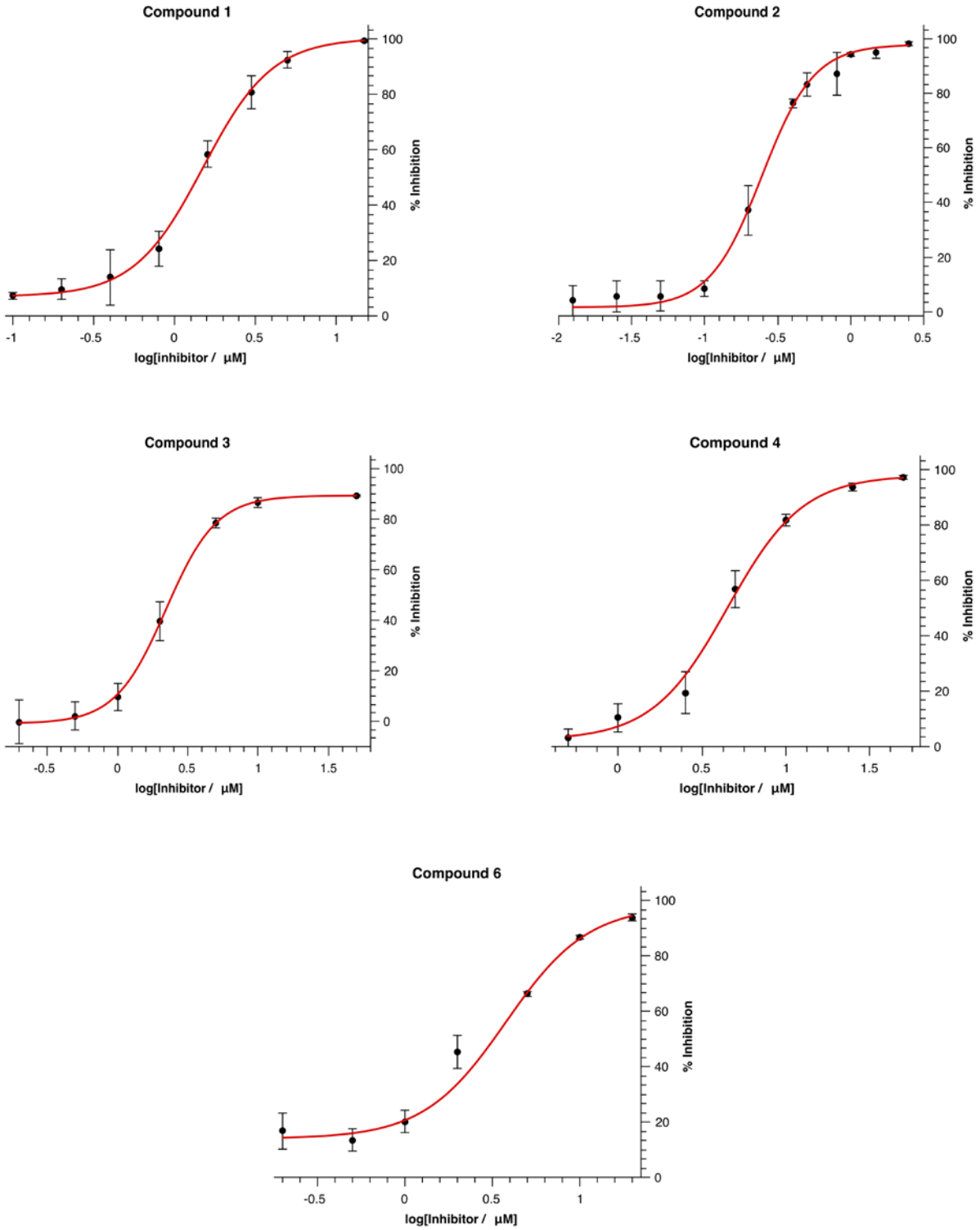

Figure S6. Dose response curves of Zika virus NS2B-NS3 protease inhibitors. Measurements were performed in triplicate at concentrations of 15 µM substrate and 0.5 nM unlinked Zika virus NS2B-NS3 protease (bZiPro). Dose-response curves were fitted using a sigmoid fitting function.

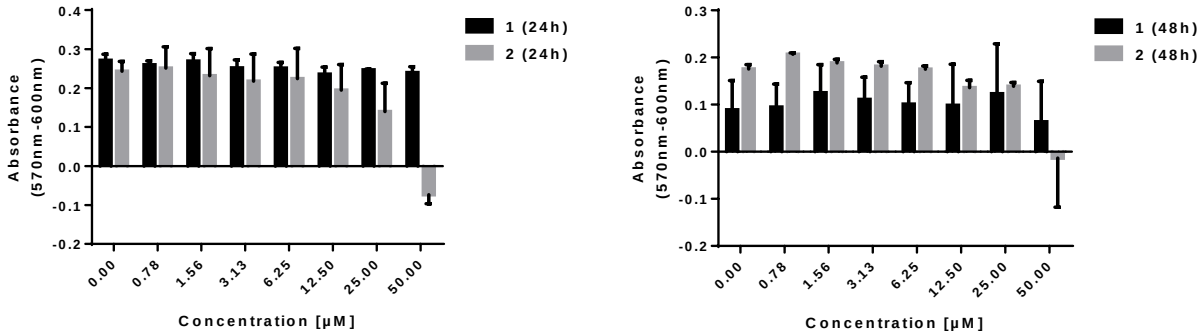

Figure S7. Absorbance data of Huh-7 cell viability assay for compounds 1 and 2. Cell viability was determined using CellTiter-Blue® reagent (Promega). The difference in absorbance at 570 nm and 600 nm is plotted against the compound concentration used for Huh-7 treatment. Measurements were performed in triplicate after 24 h (left) and 48 h (right) incubation.

Table S1. Kinetic parameters for Zika virus NS2B-NS3 protease binding of compounds identified.

Compound	k_{on} ($M^{-1} \cdot s^{-1}$)	k_{off} (s^{-1})	K_D (nM)
1	1.47×10^5	0.003	20
2	2.22×10^5	0.002	8.7
3	3.54×10^5	0.003	7.5
4	1.83×10^5	0.002	8.9
5	3.22×10^5	0.002	5.0
6*	3.04×10^4 0.004	0.042 0.001	168

* Data of compound **6** were fitted using a two-state binding model. Therefore, two values are reported for k_{on} and k_{off}.

Table S2. DNA oligonucleotides used in this work.

Name	**Sequence (5' to 3')**[a]
NNS-GT3-N8.R72	CTACGTTCCCGTTCCCGTTCCGCASNNSNNSNNSNNSNNSNNSNNCATATGTATATCTCCTTCTTAAAG
NNS-GT3-N9.R75	CTACGTTCCCGTTCCCGTTCCGCASNNSNNSNNSNNSNNSNNSNNSNNCATATGTATATCTCCTTCTTAAAG
NNS-GT3-N10.R78	CTACGTTCCCGTTCCCGTTCCGCASNNSNNSNNSNNSNNSNNSNNSNNSNNCATATGTATATCTCCTTCTTAAAG
T7g10M.F46	TAATACGACTCACTATAGGGTTAACTTTAAGAAGGAGATATACATA
CGT3an13.R23	TTTCCGCCCCCCGTCCTACGTTC
CGT3an13.R39	TTTCCGCCCCCCGTCCTACGTTCCCGTTCCCGTTCCGCA
EnGluCAU.R44	TCGAACCCCTGTTACCGCCTTATGAGGGCGGTGTCCTGGGCCTC
EnGluGUC.R44	TCGAACCCCTGTTACCGCCTTGACAGGGCGGTGTCCTGGGCCTC
EnGluCUC.R44	TCGAACCCCTGTTACCGCCTTGAGAGGGCGGTGTCCTGGGCCTC
EnGluGCG.R44	TCGAACCCCTGTTACCGCCTTCGCAGGGCGGTGTCCTGGGCCTC
EnGluCCG.R44	TCGAACCCCTGTTACCGCCTTCGGAGGGCGGTGTCCTGGGCCTC
EnGluCCU.R44	TCGAACCCCTGTTACCGCCTTAGGAGGGCGGTGTCCTGGGCCTC
Glu-5'.F49	GTAATACGACTCACTATAGTCCCCTTCGTCTAGAGGCCCAGGACACCGC
Glu-3'.R37	TGGCGTCCCCTAGGGGATTCGAACCCCTGTTACCGCC
Glu3'.R20(OMe)	TrG*GCGTCCCCTAGGGGATTC
Ini-3'.R20(OMe)	TrG*GTTGCGGGGGCCGGATTT
Ini-3'.R38	TGGTTGCGGGGGCCGGATTTGAACCGACGATCTTCGGG
Ini1-1G-5'.F49	GTAATACGACTCACTATAGGCGGGGTGGAGCAGCCTGGTAGCTCGTCGG
Ini cat.R44	GAACCGACGATCTTCGGGTTATGAGCCCGACGAGCTACCAGGCT
T7ex5.F22	GGCGTAATACGACTCACTATAG
eFx.R45	ACCTAACGCTAATCCCCTTTCGGGGCCGCGGAAATCTTTCGATCC
eFx.R18	ACCTAACGCTAATCCCCT
dFx.R46	ACCTAACGCCATGTACCCTTTCGGGGATGCGGAAATCTTTCGATCC
dFx.R19	ACCTAACGCCATGTACCCT

[a] rG* indicates 2'-O-methyl guanosine

Table S3. Non-linear least-squares fitting parameters for gZiPro (Graphpad Prism 7.0).

Compound	Non-competitive model[a]		Competitive model[b]		Mixed model[c]		
	K_i (95% CI)[d]	R^2	K_i (95% CI)[d]	R^2	K_i (95% CI)[d]	α[e] (95% CI)[d]	R^2
1	0.81 (0.68 – 0.96)	0.943	~ $1.89 \cdot 10^{-8}$ (very wide)	0.765	~ 1.47 (very wide)	~ 0.54 (very wide)	0.881
2	0.44 (0.39 – 0.50)	0.963	~ $1.26 \cdot 10^{-9}$ (very wide)	0.848	~ 0.254 (very wide)	~ 1.74 (very wide)	0.940
3	2.00 (1.65 – 2.43)	0.921	~ $2.20 \cdot 10^{-8}$ (very wide)	0.811	~ 137 (very wide)	~ 0.014 (very wide)	0.860
4	20.4 (16.9 – 24.9)	0.913	~ $5.27 \cdot 10^{-7}$ (very wide)	0.799	~ 8.75 (very wide)	~ 2.35 (very wide)	0.831
6	3.51 (2.92 – 4.24)	0.934	~ $1.07 \cdot 10^{-7}$ (very wide)	0.745	~ 7.79 (very wide)	~ 0.44 (very wide)	0.869

[a] Fitted using $v_{max}^{app} = \frac{v_{max}}{1+\frac{[I]}{K_i}}$

[b] Fitted using $K_m^{app} = K_m\left(1+\frac{[I]}{K_i}\right)$

[c] Fitted using $v_{max}^{app} = \frac{v_{max}}{1+\frac{[I]}{\alpha K_i}}$, $K_m^{app} = K_m\left(\frac{1+\frac{[I]}{K_i}}{1+\frac{[I]}{\alpha K_i}}\right)$

[d] Values for the 95% confidence interval are shown in parenthesis.

[e] Degree to which the binding of inhibitor changes the affinity of the enzyme for substrate.

References

1. Mahawaththa, M. C.; Pearce, B. J. G.; Szabo, M.; Graham, B.; Klein, C. D.; Nitsche, C.; Otting, G. Solution conformations of a linked construct of the Zika virus NS2B-NS3 protease. *Antiviral Res.* **2017,** *142*, 141-147.
2. Nitsche, C.; Mahawaththa, M. C.; Becker, W.; Huber, T.; Otting, G. Site-selective tagging of proteins by pnictogen-mediated self-assembly. *Chem. Commun.* **2017,** *53*, 10894-10897.
3. Neylon, C.; Brown, S. E.; Kralicek, A. V.; Miles, C. S.; Love, C. A.; Dixon, N. E. Interaction of the *Escherichia coli* replication terminator protein (Tus) with DNA: A model derived from DNA-binding studies of mutant proteins by surface plasmon resonance. *Biochemistry* **2000,** *39*, 11989-11999.
4. Zhang, Z.; Li, Y.; Loh, Y. R.; Phoo, W. W.; Hung, A. W.; Kang, C.; Luo, D. Crystal structure of unlinked NS2B-NS3 protease from Zika virus. *Science* **2016,** *354*, 1597-1600.
5. Goto, Y.; Ohta, A.; Sako, Y.; Yamagishi, Y.; Murakami, H.; Suga, H. Reprogramming the translation initiation for the synthesis of physiologically stable cyclic peptides. *ACS Chem. Biol.* **2008,** *3*, 120-129.
6. Hayashi, Y.; Morimoto, J.; Suga, H. *In vitro* selection of anti-Akt2 thioether-macrocyclic peptides leading to isoform-selective inhibitors. *ACS Chem. Biol.* **2012,** *7*, 607-613.
7. Jongkees, S. A. K.; Caner, S.; Tysoe, C.; Brayer, G. D.; Withers, S. G.; Suga, H. Rapid discovery of potent and selective glycosidase-inhibiting *de novo* peptides. *Cell Chem. Biol.* **2017,** *24*, 381-390.
8. Matsunaga, Y.; Bashiruddin, N. K.; Kitago, Y.; Takagi, J.; Suga, H. Allosteric inhibition of a semaphorin 4D receptor plexin B1 by a high-affinity macrocyclic peptide. *Cell Chem. Biol.* **2016,** *23*, 1341-1350.
9. Passioura, T.; Watashi, K.; Fukano, K.; Shimura, S.; Saso, W.; Morishita, R.; Ogasawara, Y.; Tanaka, Y.; Mizokami, M.; Sureau, C.; Suga, H.; Wakita, T. *De novo* macrocyclic peptide inhibitors of hepatitis B virus cellular entry. *Cell Chem. Biol.* **2018,** *25*, 906-915.

10. Song, X.; Lu, L. Y.; Passioura, T.; Suga, H. Macrocyclic peptide inhibitors for the protein-protein interaction of Zaire Ebola virus protein 24 and karyopherin alpha 5. *Org. Biomol. Chem.* **2017,** *15*, 5155-5160.
11. Yamagishi, Y.; Shoji, I.; Miyagawa, S.; Kawakami, T.; Katoh, T.; Goto, Y.; Suga, H. Natural product-like macrocyclic N-methyl-peptide inhibitors against a ubiquitin ligase uncovered from a ribosome-expressed *de novo* library. *Chem. Biol.* **2011,** *18*, 1562-1570.
12. Goto, Y.; Katoh, T.; Suga, H. Flexizymes for genetic code reprogramming. *Nat. Protoc.* **2011,** *6*, 779-790.
13. Lei, J.; Hansen, G.; Nitsche, C.; Klein, C. D.; Zhang, L.; Hilgenfeld, R. Crystal structure of Zika virus NS2B-NS3 protease in complex with a boronate inhibitor. *Science* **2016,** *353*, 503-505.
14. Becker, W.; Adams, L. A.; Graham, B.; Wagner, G. E.; Zangger, K.; Otting, G.; Nitsche, C. Trimethylsilyl tag for probing protein-ligand interactions by NMR. *J. Biomol. NMR* **2018,** *70*, 211-218.
15. Nitsche, C.; Schreier, V. N.; Behnam, M. A.; Kumar, A.; Bartenschlager, R.; Klein, C. D. Thiazolidinone-peptide hybrids as dengue virus protease inhibitors with antiviral activity in cell culture. *J. Med. Chem.* **2013,** *56*, 8389-8403.
16. Nitsche, C.; Zhang, L.; Weigel, L. F.; Schilz, J.; Graf, D.; Bartenschlager, R.; Hilgenfeld, R.; Klein, C. D. Peptide–boronic acid inhibitors of flaviviral proteases: medicinal chemistry and structural biology. *J. Med. Chem.* **2017,** *60*, 511-516.